Role of zinc coat in friction stir lap welding Al and zinc coated steel

Y. C. Chen*[1], T. Komazaki[2], T. Tsumura[1] and K. Nakata[1]

AC4C cast Al alloy and Zn coated steel were successfully lap welded using friction stir welding technology. Full strength joints could be obtained and the joints fractured at Zn coated steel base metal side, while Al alloy and unzinced steel could not be welded in the same welding conditions. The joining mechanism and the role of Zn coat on friction stir lap welding of Al alloy and Zn coated steel were put forward. The intervention of Zn coat promoted the formation of Al–Zn low melting point eutectic structure at the interface, which significantly improved the weldability of Al and steel.

Keywords: Friction stir welding, Al alloys, steels

Introduction

As a solid state welding technology, friction stir welding (FSW) process[1] can weld many materials such as Al alloys,[2–7] Mg alloys,[8,9] Ti alloys,[10,11] steels[12,13] and composite materials[14] and can get high quality joints than fusion welding technology. Such good merits are also expected for joining dissimilar materials. The need of light weight and excellent corrosion resistance in automotive body construction lead to the increasing use of the combination of Al alloy and Zn coated steel in fabrication of vehicles.[15,16] Therefore, development of reliable joints between Al alloy and Zn coated steel was required. However, from present researching status of FSW Al and steel, the majority studies were focused on FSW of Al alloy and unzinced steel[17–31] and the minority researches had involved FSW of Al alloy and Zn coated steel.[32,33] From the industrial application point of view, developing FSW of Al and Zn coated steel is necessary.

Up to date, researches on FSW of Al and unzinced steel mainly included three aspects, i.e. butt joint researches, spot joint researches and lap joint researches; studies on FSW of Al and Zn coated steel only involved lap joint researches.

Studies on friction stir butt welding (FSBW) Al and unzinced steel were the main trend in current researches.[17–26] Unlike in FSBW Al alloys, the offset of pin relative to the butt line exerted a significant effect on weld quality for FSBW of Al and steel. Watanabe and co-workers[17–19] investigated the friction stir weldability of 5083 Al and SS400 steel. The maximum tensile strength of a joint could reach 86% of that of Al base metal at the pin thrust distance of 0·2 mm toward steel. Similarly, Yasui and co-workers[22,23] investigated the weldability of 6063-T6 Al and S45C steel via FSBW and showed that the tensile strength of a joint could reach 75% of that of Al base metal at an offset of 0·05 mm toward steel. Kimapong *et al.*[24] studied the FSBW feasibility of joining 6061 Al to mild steel. They reported that pin position relative to butt line exerted a significant effect on the microstructure and tensile properties of the joints. When 90% of the pin diameter was offset into the Al side, the weld exhibited maximum tensile strength of 240 MPa, which was 86% of the Al base metal tensile strength. When the pin was moved into the Al side completely, the tensile strength of the welds decreased. Chen and Kovacevic[25] investigated the effect of the offset of pin position on the weld quality and showed that an offset of 68% of the pin diameter into the Al side led to a better weld quality. In addition, in FSBW Al and steel joints, some researches identified steel fragments and Al–Fe intermetallic compounds,[17,25,26] while others showed different results.[22] For example, intermetallic compounds of Al13Fe4 and Al5Fe2 were detected in FSBW 6061-T6 and AISI 1018 steel joints.[25] A layer of Al4Fe with thickness of 250 nm was found in FSBW 6056-T4 Al and 304 A steel joints.[26] However, Yasui and co-workers' analysis results about high speed FSBW 6063-T6 Al and S45C steel showed that no intermetallic compounds were formed in the joint. In their experiments, the maximum welding speed was 1000 mm min^{-1}.[22]

Studies on friction stir spot welding (FSSW) of Al and steel were relative lack.[27, 28] Tanaka. K and co-workers studied the FSSW feasibility of Al sheet and mild steel sheet.[27] They reported that high strength joint was obtained by stirring Al alloy near the interface without inserting a welding tool to steel surface from the Al alloy side. The strength of FSSW joint was higher than that of resistance spot welds. No brittle intermetallic compound was observed at the weld interface besides a thin amorphous layer.

As for friction stir lap welding (FSLW) of Al and steel, the interface microstructure evolution, mechanical properties of joints and the effect of parameters on weld quality were investigated.[29–31] Elrefaey *et al.* studied the feasibility of FSLW a commercially pure Al plate to a low carbon steel plate and investigated the effects of the

[1]Joining and Welding Research Institute, Osaka University, 11 1 Mihogaoka, Ibaraki, Osaka 567 0047, Japan
[2]Ryobi Limited, 5 2 8 Toshima, Kita ku, Tokyo 114 8518, Japan

*Corresponding author, email armstrong@hit.edu.cn

Published by Maney on behalf of the Institute
Received 18 July 2007; accepted 7 September 2007
DOI 10.1179/174328407X248505

welding parameters on the joint strength.[29] It was reported that the joint strength depended strongly on the depth of the pin tip relative to the steel surface; when the pin depth did not reach the steel surface, the joint failed under low applied loads. Meanwhile, slight penetration of the pin tip to the steel surface significantly increased the joint strength. Kimapong and Watanabe reported the results about FSLW of 5083 Al and SS400 steel.[30,31] They showed that the joint shear strength decreased with increasing a tool tilt angle and a pin diameter due to the formation of a thick Al5Fe intermetallic compound layer at the joint interface. But the presence of a prehole, which was opened at the pin inserting position of an Al plate before welding, was helpful to obtain the higher shear strength of the joints. The optimal prehole indicated the shear strength of ~77% that of the Al base metal. The interface microstructure examination showed that no intermetallic compound was formed at the joint interface.

Although previous investigations showed that the weld quality of FSW of Al and steel was difficult to control because of the formation of some intermetallic compounds at the weld interface, some recent attempts had demonstrated a success in joining Al and Zn coated steel using FSLW.[32,33] The adoption of Zn coated steel evidently improved the friction stir weldability of Al and steel and the full strength joints could be obtained.[32] Ahmed *et al*. investigated the weldability of 1100H24 Al alloy and Zn coated steel using FSW.[33] They found that the Al/Zn coated steel joint exhibited considerable fracture load at probe depth of 2·0 mm, while Al/steel joints were so weak that they fractured during preparation of the specimen for metallographic analysis at the same probe depth. They considered that Zn played a role of lubricant in the friction between Al alloy and steel substrate.

Current reporting literatures were mainly focused on the processing investigations on FSLW of Al alloy and Zn coated steel. The study of the joining mechanism on FSLW of Al alloy and Zn coated steel was limit, especially the study about the role of Zn coat in FSLW of Al alloy and Zn coated steel. Studies on this topic are important for us not only to reveal the friction stir weldabilities of Al alloy and Zn coated steel but also to comprehend the effect of coated metal on the friction stir weldability of dissimilar materials.

In the present study, AC4C cast Al alloy and low carbon Zn coated steel are selected as the experimental materials for FSLW. The Al alloy sheet is put on the Zn coated steel sheet. The insert depth of the tool is strictly controlled less than the thickness of the Al alloy. That is, the probe tip of the tool does not reach the surface of the Zn coated steel sheet during welding. The emphasis is to study the interface microstructure evolution and clarify the joining mechanism and the role of Zn coat on FSW of Al and Zn coated steel.

Experimental

The base materials used in the present study were a 3 mm thick AC4C cast Al alloy sheet and a 0·8 mm thick low carbon Zn coated steel sheet. For comparison, the same thickness low carbon steel sheets without Zn coat were selected as experimental materials. The chemical compositions and mechanical properties of the base materials are shown in Table 1. Rectangular welding samples, 300 mm long by 100 mm wide, were longitudinally lap welded using an FSW machine. After a series of feasibility tests, following experimental parameters were selected in the present study. The welding parameters are rotation speed of 1500 rev min^{-1} and welding speed of 60–120 mm min^{-1}. The upsetting force of the welding tool (made of SKD61 steel) is 1 ton. The shoulder diameter and probe diameter of the tool are 15 and 5 mm respectively. The length of the probe is 2·9 mm and the welding tilt angle is 3°.

After welding, the joint was cross-sectioned perpendicular to the welding direction for the metallographic analyses and tensile tests using an electrical discharge cutting machine. The cross-sections of the metallographic specimens were polished with diamond polishing agent, etched with Keller's reagent (1 mL hydrochloric acid, 1·5 mL nitric acid, 2·5 mL hydrofluoric acid and 95 mL water) and observed by optical microscopy. Because Al alloy and unzinced steel could not be welded in current experimental conditions, metallographic analysis specimens could not be prepared. The details of tensile test specimens and tensile test results of FSW joints of AC4C and Zn coated steel referred to Ref. 32.

In order to determine the microstructure evolution along the lap interface of Al alloy and Zn coated steel, a three-dimensional rectangular coordinate system was established in the cross-section plane of a typical joint. The X axis is across the weld from the advancing side (AS) to the retreating side (RS), the Y axis is through the thickness of the joint from the steel side to the Al side, and the Z axis is in the direction of welding. X axis is the lap interface and Y axis passes the centre of the weld. On the other hand, for the sake of observing the joining state from another angle, all the joints were separated by manual manipulation. In this way, the joining status of the lap interface could be directly observed from the front face. The widths of joining regions at different welding parameters are shown in Table 2. Fracture surfaces of joints were analysed using X-ray diffraction.

The welding thermal cycle histories along the interface during FSW were measured with an array of K type thermocouples (0·2 mm diameter) at various locations distant from the weld centre. Microstructure characteristic and element distribution along the interface were analysed by scanning electron microscopy equipped with an energy dispersive X-ray spectroscopy analysis system.

Table 1 Chemical compositions and mechanical properties of base materials

	Chemical compositions, mass-%										Mechanical properties	
Base materials	Al	Cu	Mn	Fe	C	Mg	Ni	P	Si	S	Strength, MPa	Elongation, %
AC4C	Bal.	0·05	0·3	0·15	–	0·2	–	–	7·5	–	244	7·4
Zn coated steel	0·06	0·02	0·20	Bal.	0·04	–	0·01	0·013	–	0·005	328	33·4

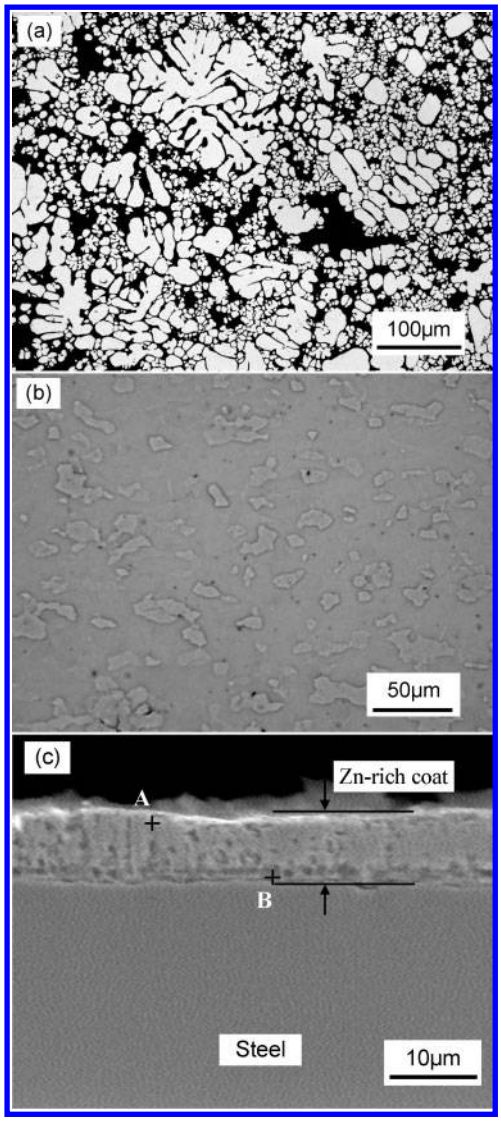

a AC4C Al alloy; *b* steel; *c* Zn coat

1 Microstructure of base material

Results and discussion

Figure 1 shows the microstructure of the base materials. AC4C base material is a hypoeutectic Al–Si alloy showing a typical hypoeutectic structure. The steel base material shows ferritic structure due to low carbon content. Figure 1*c* shows the microstructure near the Zn coat surface. It can be seen from this figure that the thickness of Zn coat is ~10 μm. Moreover, because this kind of Zn coat is produced using hot dip galvanising process, actually the Zn coat is composed of Fe–Zn intermetallic compounds.[34] Elements analysis was performed at different position of Zn rich coat. The chemical composition of points A and B are 75·06

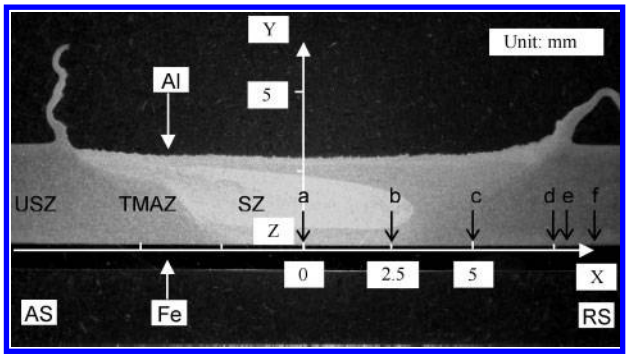

2 Typical cross-section of lap joint

Zn–20·73Fe–4·21Al and 62·91Zn–34·95Fe–2·15Al (at.-%) respectively. The dominant element in Zn coat is Zn and iron. Moreover, the content of Zn increases with approaching the surface of layer. That is to say, the composition of layer more and more approaches pure Zn from the interface to the surface.

Tensile test results[32] show that the welding speed has a significant effect on the mechanical properties of Al and Zn coated steel friction stir lap joints at rotation speed of 1500 rev min^{-1}. When the welding speed is 60 mm min^{-1}, the joints fracture at the interface; when the welding speed is >80 mm min^{-1}, all the joints fracture at steel base metal side. It means that full strength Al and Zn coated steel friction stir lap joints can be obtained when the welding parameters are selected in reason. However, when the authors use the same welding conditions to weld Al alloy and unzinced steel, they can not be welded. These results indicate that the presence of Zn rich coat greatly improves the friction stir lap weldability of Al and steel.

Figure 2 shows a typical transverse cross-section of a joint at the welding speed of 100 mm min^{-1} and a corresponding rectangular coordinate system. It can be seen from this figure that Al and steel are joined tightly and the microstructure characteristic in Al side is similar to that of FSW of Al alloy itself. That is, the typical stir zone (SZ), thermomechanically affected zone (TMAZ) and unstir zone (USZ) are observed. In this case, the authors are mainly interested in the interface structure feature and observe half of the interface microstructure from the central line because the microstructure in AS and RS is approximately symmetric distribution. Microstructure observations start from the centre of the weld (point a) and end the base material zone (point f). The details of the microstructural variations are demonstrated in Fig. 4.

Figure 3 shows the joining state of a joint at steel side in Y direction after the joint is separated by manual manipulation. From this figure we can see that four significant zones are produced after welding. For convenience, the authors define the four zones as zone 1 to zone 4 from the centre of the weld to the base material according to the characteristic of different

Table 2 Relationships between widths of different zones and welding speeds

	AS		Centre	RS		AS + Centre + RS
Speed, mm min^{-1}	Zone 3	Zone 2	Zone 1	Zone 2	Zone 3	Total width
60	2 mm	2·5 mm	12 mm	2·5 mm	2 mm	21 mm
80	2 mm	1·5 mm	12·5 mm	1·5 mm	2 mm	19·5 mm
100	1·8 mm	1 mm	13·5 mm	1 mm	2 mm	19·3 mm
120	1·5 mm	1 mm	13 mm	1 mm	1·5 mm	18 mm

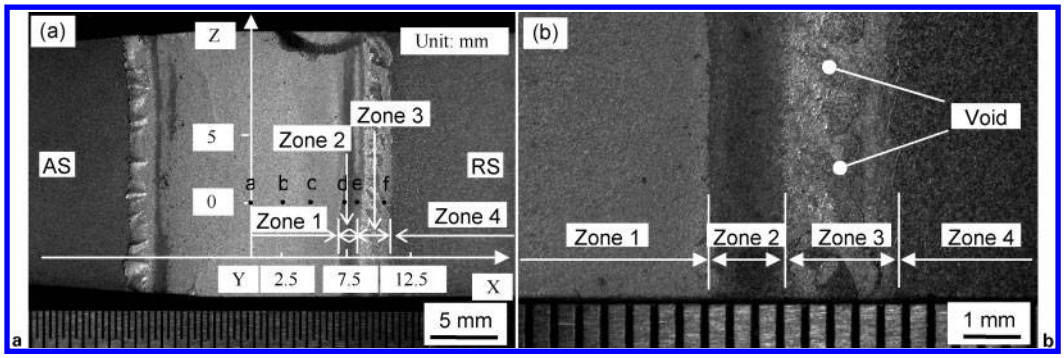

a low magnification; *b* high magnification

3 Macrostructure of fracture surface at steel side

regions. In addition, the corresponding location of microstructure analysis from point a to point f is shown in X–Z rectangular coordinate system.

From the characteristic of the fracture and following microstructure analysis the authors can confirm that zone 1 is a typical reaction region. The width of this region obviously exceeds that of the probe diameter. The authors call it combination reaction region (CRR). Zone 2 is a narrow transition region (TR). Zone 3 shows resolidifying characteristic. Moreover, liquid flow trace can be seen from front side. Some voids remain in this region because of insufficient flow behaviour (see Fig. 3*b*). From following structure analysis we can know that zone 3 is an eutectic structure zone. The authors call it eutectic reaction region (ERR). Zone 4 is the base material (BM). Relationships between widths of different zones and welding speeds are listed in Table 2.

From Table 2 we can find that the width of CRR changes between 12 and 13·5 mm. Such values obviously exceed that of the probe diameter. The width of TR changes from 1 to 2·5 mm. The width of ERR is ~2 mm. The total width of joining region (CRR + TR + ERR) changes between 18 and 21 mm, which is wider than that of the shoulder diameter. Moreover, the lower the welding speeds, the wider the total width.

Figure 4 shows the details of the microstructural variations mentioned in Figs. 2 and 3. It can be seen from Fig. 4*a* that the joint consists of a four layered structure, i.e. microstructure in SZ of Al alloy, a new

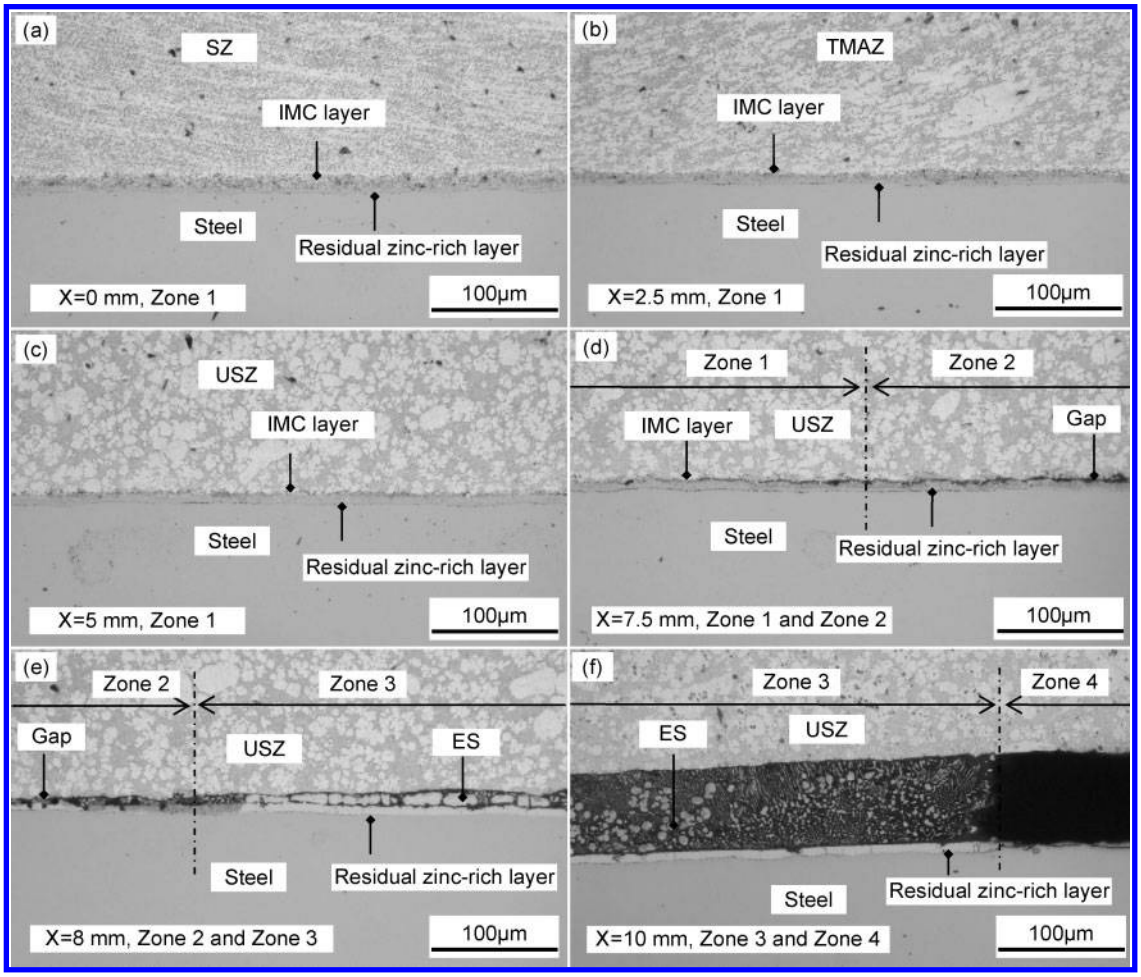

4 Microstructure distributions along interface

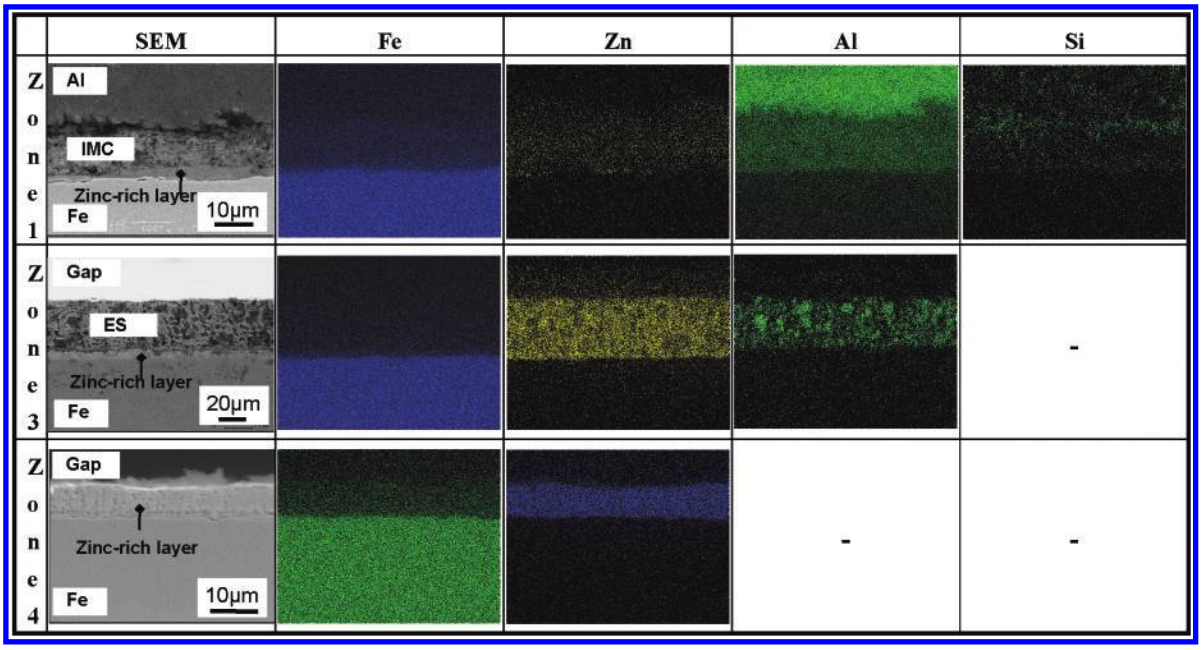

5 Elements distributions in different zones (welding speed, 100 mm min^{-1})

intermetallic compound (IMC) layer, residual Zn rich layer and BM of steel. Al alloy and steel are joined through intermediate reaction zone. Between the residual Zn rich layer and SZ of Al alloy, there is a new IMC layer. That is to say, the original Zn rich coat is partially replaced by a new IMC layer at the interface after welding. Figure 4*b* shows the microstructure in TMAZ. The interface structure is similar to that in Fig. 4*a*. But the thickness of IMC is thinner than that in SZ. Figure 4*c* shows the microstructure in USZ. This region is far from the SZ but still under the shoulder. The interface microstructure in this region is significantly different from that in SZ. The four layers structure mentioned above are still present. The thickness of IMC layer, however, explicitly decreases compared with those in SZ and TMAZ. Most of Zn rich coat is remained. The thickness of residual Zn rich layer is similar to that of original Zn coat. Figure 4*d* shows the adjacent position between zone 1 and zone 2. No significant intermetallic compound is found in zone 2 besides a gap. Zone 2 is the start position that Al alloy and Zn coated steel are in unbound state. The position is near Y axis position of the edge of shoulder diameter. Figure 4*e* shows the adjacent position between zone 2 and zone 3. A typical eutectic structure (ES) is found in zone 3. The ES fills into the clearance between Al alloy and Zn coated steel. Figure 4*f* shows the adjacent position between zone 3 and zone 4. The position of Fig. 4*f* has greatly exceeded the domain of shoulder diameter of the tool. The thickness of ES significantly increases because of the larger clearance between two sheets.

Figure 5 shows the representative concentration profiles of Al, Si, Zn and Fe cross the interface at different zones between Al alloy and Zn coated steel by a map scanning element analysis. A layer involving Al, Fe, Zn and Si is formed at the interface of the joint in zone 1. X-ray diffraction analysis results from fracture surface show that Fe2Al5 and Fe4Al13 are the main compounds at the interface. More exact analysis to the IMC will perform using TEM in the future. Results from zone 3 show that the concentration profiles of Al and Zn is detected in the ES layer, which indicates that zone 3 is an Al–Zn eutectic structure region. Results from zone 4 show the distribution of Zn and Fe in original Zn rich coat on the surface of steel. As mentioned above, actually this kind of Zn rich coat is composed of Zn and Fe.

In order to further clarify the joining mechanism, welding heat cycle histories are measured with an array of K type thermocouples during welding as shown in Fig. 6. It is notable from above interface structure analysis results that the position of 8 mm is the location of zone 3. The welding heat cycle history results are shown in Fig. 7. The peak temperatures at positions of 0, 8 and 20 mm are 449, 388 and 239°C respectively. Figure 8 shows an Al–Zn binary phase diagram.[35] The melting point of Al and Zn is 660 and 420°C respectively. The binary eutectic temperature of Al–Zn is 381°C at Zn rich corner. In other words, the peak temperature in the lap interface centre is higher than those of Zn melting point and Al–Zn eutectic point. The peak temperature in zone 3, i.e. near Y axis position of the edge of shoulder, is almost the same to the eutectic

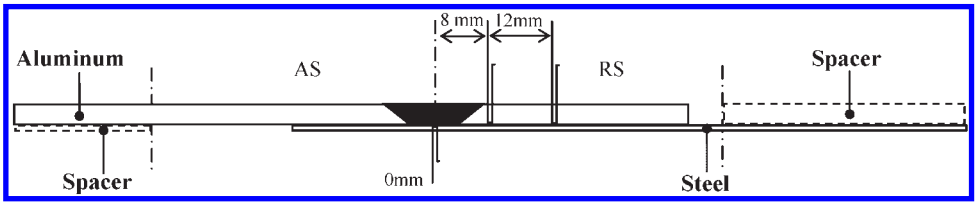

6 Temperature measure method and locations

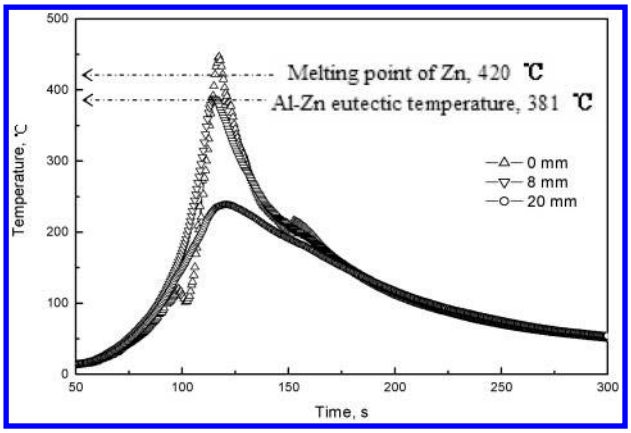

7 Welding heat cycle history at different locations (welding speed, 100 mm min^{-1})

temperature of Al–Zn. Moreover, from the welding heat cycle history we can know that the high temperature dwell time above Zn melting point and Al–Zn eutectic point is about 4 and 9 s in the lap interface centre. The high temperature dwell time above Al–Zn eutectic point is ~3·5 s in zone 3. It means that liquid Al–Zn eutectic structure can be formed because of high peak temperature and has enough time to fill into the clearance between two sheets. Moreover, the appearance of eutectic structure in zone 3 also indicates that Al–Zn reaction layer is present from the centre of weld to the Y axis position of the edge of shoulder. The intervention of Zn coat directly promotes the formation of Al–Zn low melting point eutectic structure along the interface.

According to above results, the authors put forward the following three-step joining mechanism on FSLW of Al alloy and Zn coated steel. Figures 9 and 10 show the schematic diagram of joining mechanism. Figure 9 is the macroscopic schematic diagram of the cross-section and Fig. 10 is the corresponding microscopic schematic diagram of the interface microstructure at the weld centre. The relative position of Al, Zn rich coat and steel is shown in Figs. 9*a* and 10*a*, in which Al alloy sheet is put on the Zn coated steel sheet with a natural clearance between them.

First, the materials in weld zone have undergone the co-action of the high temperature action and severely plastic deformation during FSW. In this way, the original coarse primary Al grains and large platelike

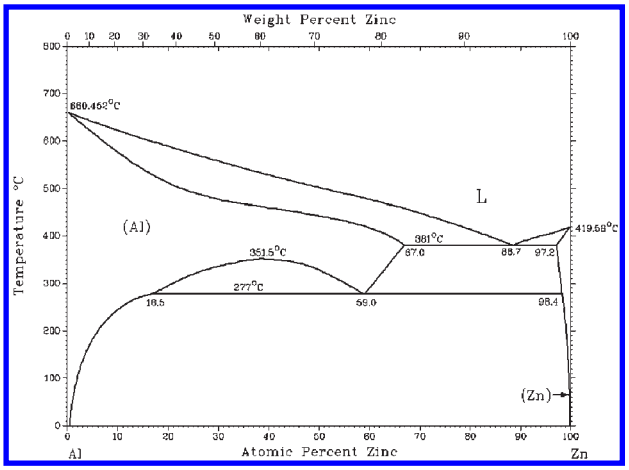

8 Al–Zn binary phase diagram[35]

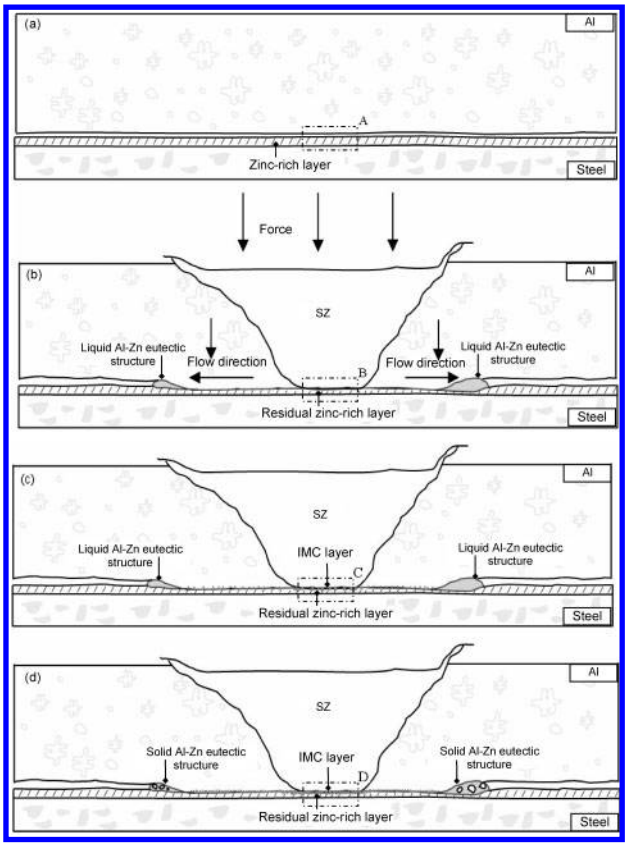

a before welding; *b* step 1; *c* step 2; *d* step 3

9 Joining mechanism macroschematic diagram of FSLW Al and Zn coat steel

eutectic silicon in the base material have been transformed to fine grains and small silicon particles in the SZ. The metal in the lap interface simultaneously undergoes the synthetic effect of the thermal cycle and the mechanical cycle because of the action of friction, stir and extrusion of the tool. Thus, high temperature and high pressure are generated at the interface. High temperature firstly leads to the melting of pure Zn on the surface of Zn rich coat and high pressure simultaneously results in the rupture of surface oxide films at both sheets surface, which promotes the formation Al–Zn eutectic reaction products with lower melting point (see Fig. 10*b*). High pressure extrudes excessive liquid phase of Al–Zn eutectic reaction product with broken oxide films and surface contamination far from the weld centre, spreads along the interface till piles into the natural clearance between two sheets (see Fig. 9*b*). The final position of the liquid Al–Zn eutectic phase can reach near Y axis position of the edge of shoulder, where the peak temperature is almost the same to the Al–Zn eutectic temperature.

Second, the fresh interfaces of Al and residual Zn rich layer are exposed and they are tightly extruded together after liquid eutectic phase is pushed out. Elements mutual diffusion of Al and iron occurs, which leads to the formation of a new intermetallic compound layer adjacent to the lap interface of the weld (see Figs. 9*c* and 10*c*). The thickness of IMC layer increases with increasing weld time (see Figs. 9*d* and 10*d*).

Thirdly, during the cooling after welding, liquid Al–Zn eutectic phase transforms to solid eutectic structure (see Fig. 9*d*).

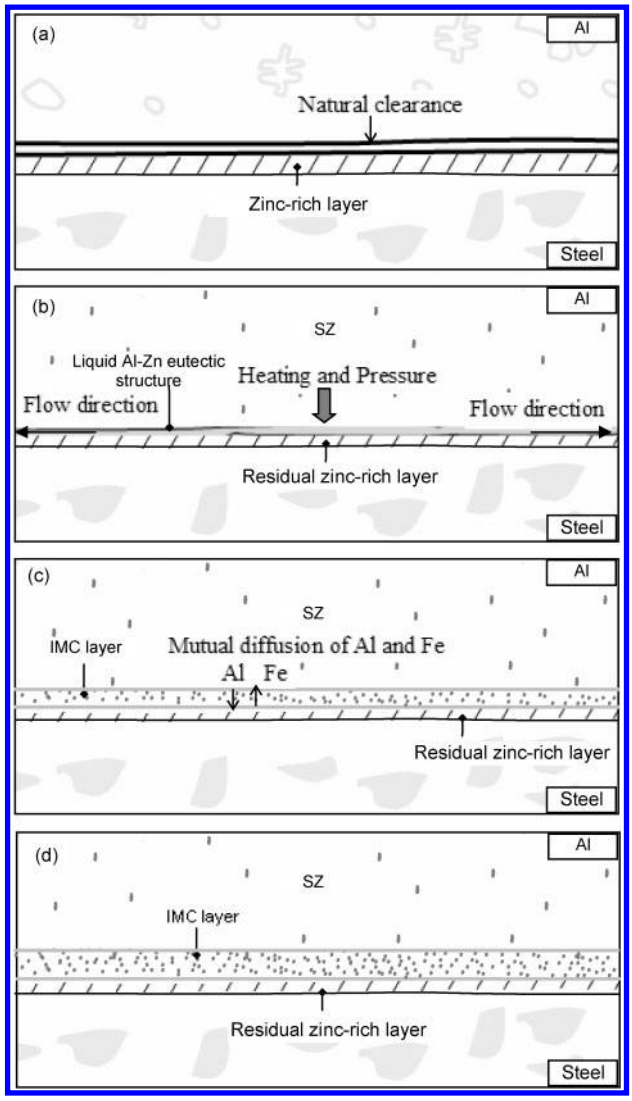

a region A in Fig. 9*a*; *b* region B in Fig. 9*b*; c region C in Fig. 9c; *d* region D in Fig. 9*d*

10 Joining mechanism microschematic diagram of interface structure at weld centre

In brief, the presence of Zn directly results in the formation of Al–Zn low melting point eutectic structure along the interface, which significantly improved the weldability of Al and steel.

Conclusions

AC4C cast Al alloy and Zn coated steel were successfully lap welded using FSW technology. The microstructure evolution and the temperature distributions along the interface were investigated. The joining mechanism on FSLW of Al alloy and Zn coated steel was put forward. The main viewpoints were shown as following.

The joint contained four different structure zones along the lap interface, i.e. combination reaction region, transition region, eutectic reaction region and the base material; the joint consisted of four layers structure vertical to the lap interface, i.e. microstructure in stir zone of Al alloy, a new intermetallic compound layer, residual Zn rich layer and base material of steel.

The peak temperature in the lap interface centre was higher than those of Zn melting point and Al–Zn eutectic point. High temperature led to the melting of Zn rich coat and promoted the formation of lower melting point Al–Zn eutectic reaction product. Liquid state Al–Zn eutectic reaction product was extruded far from the weld centre, spread along the interface till piled into the natural clearance between two sheets. A new intermetallic compound layer was simultaneously formed at the interface. During the cooling after welding, liquid state Al–Zn eutectic reaction product transformed to solid eutectic structure.

References

1. C. J. Dawes and W. M. Thomas: *Weld. J.*, 1996, **75**, 41–45.
2. Y. Chen, H. Liu and J. Feng: *Mater. Sci. Eng. A*, 2006, **A420**, 21–25.
3. H. J. Liu, Y. C. Chen and J. C. Feng: *Mater. Sci. Technol.*, 2006, **22**, 237–241.
4. Y. S. Sato, H. Kokawa, M. Enomoto and S. Jogan: *Metall. Mater. Trans. A*, 1999, **30A**, 2429–2437.
5. J. C. Feng, Y. C. Chen and H. J. Liu: *Mater. Sci. Technol.*, 2006, **22**, 86–90.
6. H. J. Liu, Y. C. Chen and J. C. Feng: *Scr. Mater.*, 2006, **55**, 231–234.
7. Y. C. Chen, H. J. Liu and J. C. Feng: *J. Mater. Sci.*, 2006, **41**, 297–299.
8. X. H. Wang and K. S. Wang: *Mater. Sci. Eng. A*, 2006, **A431**, 114–117.
9. W. B. Lee, Y. M. Yeon and S. B. Jung: *Mater. Sci. Technol.*, 2003, **19**, 785–790.
10. A. J. Ramirez and M. C. Juhas: *Mater. Sci. Forum*, 2003, **426–432**, 2999–3004.
11. W. B. Lee, C. Y. Lee, W. S. Chang, Y. M. Yeon and S. B. Jung: *Mater. Lett.*, 2005, **59**, 3315–3318.
12. L. Cui, H. Fujii, N. Tsuji and K. Nogi: *Scr. Mater.*, 2007, **56**, 637–640.
13. H. Fujii, L. Cui, N. Tsuji, M. Maeda, K. Nakata and K. Nogi: *Mater. Sci. Eng. A*, 2006, **A429**, 50–57.
14. H. Uzun: *Mater. Design*, 2007, **28**, 1440–1446.
15. G. Kobe: *Chilton's Autom. Industr.*, 1994, **174**, 44.
16. S. Ramasamy: *Weld. J.*, 2000, **79**, 35–39.
17. T. Watanabe, H. Takayama and A. Yanagisawa: *J. Mater. Proc. Technol.*, 2006, **178**, 342–349.
18. T. Watanabe, H. Takayama, K. Kimapong and N. Hotta: *Mater. Sci. Forum*, 2003, **426–432**, 4129–4134.
19. T. Watanabe, H. Takayama, A. Yanagisawa and S. Konuma: *Q. J. Jpn Weld. Soc.*, 2005, **23**, 603–607.
20. W. H. Jiang and R. Kovacevic: *J. Eng. Manufact.*, 2004, **218**, 1323–1331.
21. U. Huseyin, D. D. Claudio, A. Alberto, G. Tommaso and G. Carla: *Mater. Design*, 2005, **26**, 41–46.
22. T. Yasui, Y. Shimoda, M. Tsubaki, T. Ishii and M. Fukumoto: *Q. J. Jpn Weld. Soc.*, 2005, **23**, 469–475.
23. T. Yasui, Y. Shimoda, M. Tsubaki and M. Fukumoto: *Mater. Sci. Forum*, 2004, **449–452**, 433–436.
24. K. Kimapong and T. Watanabe: *Weld. J.*, 2004, **83**, 277–282.
25. C. M. Chen and R. Kovacevic: *Int. J. Mach. Tool. Manufact.*, 2004, **44**, 1205–1214.
26. W. B. Lee, M. Schmuecker, U. A. Mercardo, G. Biallas and S. B. Jung: *Scr. Mater.*, 2006, **55**, 355–358.
27. K. Tanaka, M. Kumagai and H. Yoshida: *J. Jpn Inst. Light Met.*, 2006, **56**, 317–322.
28. J. Barnes: *Adv. Mater. Proc.*, 2005, **163**, 29.
29. A. Elrefaey, M. Gouda, M. Takahashi and K. Ikeuchi: *J. Mater. Eng. Perf.*, 2005, **14**, 10–17.
30. K. Kimapong and T. Watanabe: *Mater. Trans.*, 2005, **46**, 2211–2217.
31. K. Kimapong and T. Watanabe: *Mater. Trans.*, 2005, **46**, 835–841.
32. Y. C. Chen, T. Komazaki, Y. G. Kim, T. Tsumura and K. Nakata: Proc. Int. Conf. on 'Welding and joining', Seoul, Korea, May 2007, The Korean Welding and Joining Society, SB1–2.
33. E. Ahmed, T. Makoto and I. Kenji: *Q. J. Jpn Weld. Soc.*, 2005, **23**, 186–193.
34. A. R. Marder: *Prog. Mater. Sci.*, 2000, **45**, 191–271.
35. J. L. Murray: In 'Binary alloy phase diagram', (ed. T. B. Massalski), 185; 1986, Materials Park, OH, ASM.